Hence only two of the three parameters are independent. Because of the scaling relations in Eqs. (11–152) and (11–154), a change in the operating frequency changes only the particular dipole whose length is a certain fraction of a wavelength.† The remarks pertaining to Eqs. (11–150), (11–151a), and (11–151b) apply, and we have a log-periodic dipole array.

The array is usually fed by a source connected to a transmission line. An important discovery is that neighboring elements must be fed at opposite phases. This is accomplished by transposing the wires of the transmission line leading to alternate dipoles, as illustrated in Fig. 11–30. At the operating frequency the active region of the array consists mainly of the several dipoles whose lengths are approximately a half-wavelength and where the dipole currents are large. The currents in the dipoles outside this region are relatively very small. The array operates in an end-fire fashion with its main beam of radiation in the direction of short dipoles.

11–9 Aperture Radiators

Our analysis of the radiation characteristics of antennas has generally proceeded from a current distribution on the antenna structure. From the current distribution the retarded vector potential is determined by using Eq. (11–3). The magnetic and electric field intensities can then be found from Eqs. (11–1) and (11–6), respectively. In many cases, electromagnetic radiation may be viewed as emanating from an opening or an aperture in a conducting enclosure. To be sure, the source of radiation can always be traced to some time-varying currents somewhere; but the current distributions are often unknown and difficult to determine or approximate. Such radiating systems are quite unlike dipole antennas and must be analyzed in a different way. They are aperture radiators or aperture antennas. Examples are slots, horns, reflectors, and lenses, some of which are illustrated in Fig. 11–31.

In our analysis we will use an approximate aperture-field method, assuming that electric and magnetic fields exist only in the aperture area and that the field elsewhere in an infinite screen containing the aperture is zero. In the case of the slot radiator shown in Fig. 11–31(a), the field for dominant TE_{10}-mode excitation is usually assumed to be a half-sine having a maximum at the center of the slot and tapering to zero at the edges. For the horn in Fig. 11–31(b) the aperture field is derived from the waveguide mode propagating into a horn of infinite extent. The aperture fields of the reflector in Fig. 11–31(c) and the lens in Fig. 11–31(d) are found by methods of geometrical optics from the reflection and refraction of rays emanating from the primary feed.

For TE_{10}-mode excitation the field in a plane aperture is approximately linearly polarized, and deviations from the results obtained by geometrical optics are small.

† Strictly speaking, it is also necessary to scale the radius a_n of the dipoles according to $a_{n+1}/a_n = \tau$.

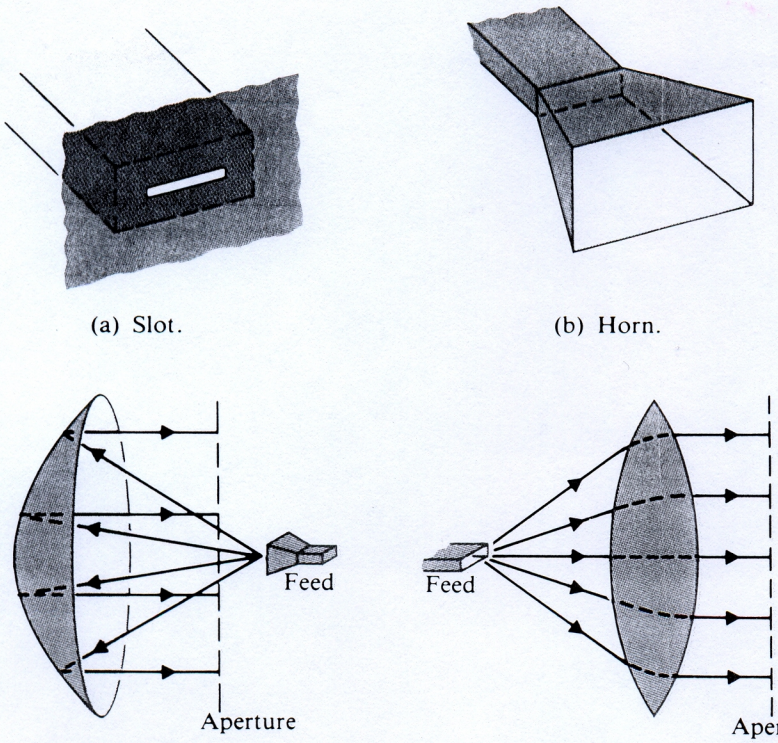

(a) Slot. (b) Horn. (c) Reflector. (d) Lens.

FIGURE 11–31
Aperture antennas.

With a nearly uniform phase over the aperture, the far-zone field is a two-dimensional Fourier integral of the field distribution in the aperture. Let the electric field distribution in the aperture outlined in Fig. 11–32 be linearly polarized, say in the x-direction, with no phase variation:

Boundary Condition :

$$\mathbf{E}_a = \mathbf{a}_x E_a(x, y) \tag{11–157}$$

If the aperture dimensions are large in comparison to the operating wavelength, then almost all the energy of the radiated field will be contained in a small angular region around the z-axis, and the far-zone electric field at a distant point $P(R_0, \theta, \phi)$ can be written as $\mathbf{E}_P = \mathbf{a}_x E_P$, where [13], [25]

(9-105)

$$\nabla^2 E_p + k^2 E_p = 0 \quad \nabla \cdot E_p = 0 \quad \xrightarrow[\text{Transform + (11-157)}]{\text{Fourier}} \quad E_P \cong \frac{j}{\lambda R_0} \iint_{\text{aper.}} E_a(x', y') e^{-j\beta R}\, dx'\, dy'. \tag{11–158}$$

For $\beta R \gg 1$ we have

∂_R //

$$R \cong R_0 - (\mathbf{a}_x x' + \mathbf{a}_y y') \cdot (\mathbf{a}_x \sin\theta\cos\phi + \mathbf{a}_y \sin\theta\sin\phi + \mathbf{a}_z \cos\theta)$$
$$= R_0 - (x' \sin\theta\cos\phi + y' \sin\theta\sin\phi). \tag{11–159}$$

Substitution of Eq. (11–159) in Eq. (11–158) yields

$$E_P = \frac{j}{\lambda R_0} e^{-j\beta R_0} F(\theta, \phi), \tag{11–160}$$

$\vec{E}_p = E_p \vec{a}_x$

where

$$F(\theta, \phi) = \iint_{\text{aper.}} E_a(x', y') e^{j\beta \sin\theta (x' \cos\phi + y' \sin\phi)} \, dx' \, dy' \tag{11-161}$$

is the pattern function of the aperture antenna. Equation (11–161) expresses the rather simple relation between the aperture distribution and the pattern function; namely, they are the Fourier transform of each other. The inverse relation, expressing $E_a(x', y')$ in terms of $F(\theta, \phi)$ enables us to determine the aperture field required for a specified pattern function. This is a synthesis problem.

For a rectangular aperture with dimensions $a \times b$ and separable field distributions:

$$E_a(x', y') = f_1(x') f_2(y'), \tag{11-162}$$

the pattern function in Eq. (11–161) is also separable:

$$F(\theta, \phi) = \int_{-a/2}^{a/2} f_1(x') e^{j\beta x' \sin\theta \cos\phi} \, dx' \int_{-b/2}^{b/2} f_2(y') e^{j\beta y' \sin\theta \sin\phi} \, dy'. \tag{11-163}$$

If we are interested only in the patterns in the principal planes, Eq. (11–163) can be further simplified.

1. *In the xz-plane, $\phi = 0$:*

$$\begin{aligned} F_{xz}(\theta) &= \left[\int_{-b/2}^{b/2} f_2(y') \, dy' \right] \int_{-a/2}^{a/2} f_1(x') e^{j\beta x' \sin\theta} \, dx' \\ &= C_1 \int_{-a/2}^{a/2} f_1(x') e^{j\beta x' \sin\theta} \, dx', \end{aligned} \tag{11-164}$$

where C_1 is a constant. We see that the radiation pattern in the xz-plane depends only on the aperture field distribution in the x'-direction.

2. *In the yz-plane, $\phi = \pi/2$:*

$$\begin{aligned} F_{yz}(\theta) &= \left[\int_{-a/2}^{a/2} f_1(x') \, dx' \right] \int_{-b/2}^{b/2} f_2(y') e^{j\beta y' \sin\theta} \, dy' \\ &= C_2 \int_{-b/2}^{b/2} f_2(y') e^{j\beta y' \sin\theta} \, dy', \end{aligned} \tag{11-165}$$

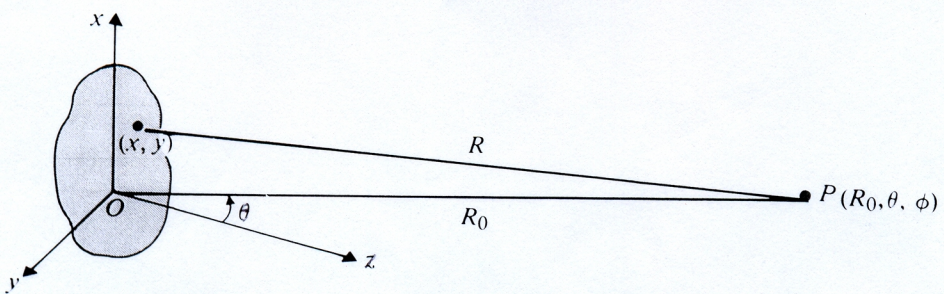

FIGURE 11–32
Pattern calculation from aperture-field distribution.

where C_2 is a constant. The radiation pattern in the yz-plane depends only on the aperture-field distribution in the y'-direction.

The directivity of an aperture radiator is obtained by using Eq. (11–35), which for convenience, is repeated below:

$$D = \frac{4\pi U_{\max}}{P_r}, \tag{11–166}$$

where

$$U_{\max} = \frac{1}{2\eta_0} R_0^2 |E_p|^2_{\max} = \frac{1}{2\eta_0 \lambda^2} \left| \iint_{\text{aper.}} E_a(x', y')\, dx'\, dy' \right|^2 \tag{11–167}$$

and

$$P_r = \text{Total power radiated} = \frac{1}{2\eta_0} \iint_{\text{aper.}} |E_a(x', y')|^2\, dx'\, dy'. \tag{11–168}$$

Combining Eqs. (11–166), (11–167), and (11–168), we have

$$D = \frac{4\pi}{\lambda^2} \frac{\left| \iint_{\text{aper.}} E_a(x', y')\, dx'\, dy' \right|^2}{\iint_{\text{aper.}} |E_a(x', y')|^2\, dx'\, dy'} \quad \text{(Dimensionless).} \tag{11–169}$$

It is interesting to note that, when $E_a(x', y') =$ a constant (uniform aperture-field distribution), D is a maximum and equals $4\pi/\lambda^2$ times the area of the aperture. This is in agreement with Eq. (11–121).

EXAMPLE 11–13 For an $a \times b$ rectangular aperture with a uniform field distribution, find (a) the pattern function in a principal plane, (b) the half-power beamwidth, (c) the location of the first nulls, and (d) the level of the first sidelobes.

Solution For simplicity we set $E_a(x', y') = 1$.

a) The pattern function in a principal plane can be found from either Eq. (11–164) or Eq. (11–165). In the xz-plane ($\phi = 0$) we have, from Eq. (11–164),

$$F_{xz}(\theta) = b \int_{-a/2}^{a/2} e^{j\beta x' \sin\theta}\, dx' = ab\left(\frac{\sin\psi}{\psi}\right), \tag{11–170}$$

where

$$\psi = \frac{\pi a}{\lambda} \sin\theta. \tag{11–171}$$

Exactly the same pattern function is obtained for $F_{yz}(\theta)$ in the other principal plane ($\phi = \pi/2$) except that b will replace a in Eq. (11–171). Note that the pattern function in Eq. (11–170) is similar to the array factor of a uniform linear array given in Eq. (11–89) when ψ is small.

b) The half-power points are determined by setting

$$\frac{\sin \psi_{1/2}}{\psi_{1/2}} = \frac{1}{\sqrt{2}},$$

from which we find

$$\psi_{1/2} = \frac{\pi a}{\lambda} \sin \theta_{1/2} = 1.39$$

or

$$\sin \theta_{1/2} = 0.442 \frac{\lambda}{a}. \tag{11–172}$$

For sufficiently large apertures, $\sin \theta_{1/2}$ is nearly equal to $\theta_{1/2}$,† and the half-power beamwidth is approximately

$$2\theta_{1/2} \cong 0.88 \frac{\lambda}{a} \quad \text{(rad)}$$

$$\cong 50 \frac{\lambda}{a} \quad \text{(deg)}.$$

c) The first null occurs at

$$\psi_{n1} = \frac{\pi a}{\lambda} \sin \theta_{n1} = \pi$$

or

$$\theta_{n1} \cong \sin \theta_{n1} = \frac{\lambda}{a} \quad \text{(rad)}. \tag{11–173}$$

d) The location of the first sidelobes is found by setting

$$\frac{\partial}{\partial \psi}\left(\frac{\sin \psi}{\psi}\right) = 0,$$

which requires $\tan \psi_1 = \psi_1$ or $\psi_1 = \pm 1.43\pi$. Thus,

$$\left|\frac{\sin \psi_1}{\psi_1}\right| = \left|\frac{\sin 1.43\pi}{1.43\pi}\right| = 0.217.$$

Referring to unity at $\psi = 0$, we find that the first sidelobes are $20 \log_{10} (1/0.217) = 13.3$ (dB) down from the level of maximum radiation. ■

† For example, when $a = 5\lambda$, $\sin \theta_{1/2} = 0.442/5 = 0.0884$ and $\theta_{1/2} = \sin^{-1}(0.0884) = 0.0885$, an error of only 0.11%. The narrow beamwidth of the main lobe confirms our previous statement that almost all of the radiated energy is confined in a small angular region around the z-axis.

EXAMPLE 11–14 A linearly polarized uniform electric field $\mathbf{E}_a = \mathbf{a}_x E_0$ exists in a circular aperture of radius b in a conducting plane at $z = 0$. Assuming b to be large in comparison to wavelength, (a) find an expression for the far-zone electric field, and (b) determine the width of the main beam between first nulls.

Solution

a) For a circular aperture we use polar coordinates $x' = \rho' \cos \phi'$, $y' = \rho' \sin \phi'$, and $x' \cos \phi + y' \sin \phi = \rho'(\cos \phi \cos \phi' + \sin \phi \sin \phi') = \rho' \cos(\phi - \phi')$. The integrand in Eq. (11–161) is to be integrated over the circular aperture. We have

$$\begin{aligned} F(\theta, \phi) &= E_0 \int_0^b \int_0^{2\pi} e^{j\beta\rho' \sin\theta \cos(\phi - \phi')} \rho' \, d\phi' \, d\rho' \\ &= E_0 \int_0^b 2\pi J_0(\beta\rho' \sin\theta) \rho' \, d\rho' \\ &= E_0 2\pi b^2 \left[\frac{J_1(\beta b \sin\theta)}{\beta b \sin\theta} \right], \end{aligned} \tag{11–174}$$

where $J_1(u)$ is the Bessel function of the first kind of the first order. The far-zone electric field is then, from Eq. (11–160),

$$\mathbf{E}_P = \mathbf{a}_x j E_0 \frac{2\pi b^2}{\lambda R_0} e^{-j\beta R_0} \left[\frac{J_1(u)}{u} \right], \tag{11–175}$$

where

$$u = \beta b \sin\theta = \frac{2\pi b}{\lambda} \sin\theta. \tag{11–176}$$

b) The first null of the radiation pattern occurs at the first zero, u_{11}, of $J_1(u)$. From Table 10–2 we find $u_{11} = 3.832$, which corresponds to an angle

$$\begin{aligned} \theta_1 &= \sin^{-1}\left(\frac{3.832\lambda}{2\pi b}\right) \cong \frac{3.832\lambda}{2\pi b} \\ &= 1.22 \frac{\lambda}{D} \quad \text{(rad)}, \end{aligned} \tag{11–177}$$

where $D = 2b$ is the diameter of the circular aperture. Hence the width of the main beam between the first nulls is $2\theta_1 = 2.44\lambda/D$ (rad). Comparing θ_1 in Eq. (11–177) with θ_{n1} in Eq. (11–173) for a rectangular aperture with width a equaling the diameter D of the circular aperture, we find that the main-lobe beamwidth for the circular aperture is wider. On the other hand, the first sidelobe level for the circular aperture is found to be 0.13, which is $20 \log_{10}(1/0.13) = 17.7$ (dB) down from the maximum radiation. This is lower than the 13.3 (dB) first sidelobes for the rectangular aperture with $a = D$. ■

† We have made use of the following two integral relations:

$$\int_0^{2\pi} e^{jw\cos\phi'} d\phi' = 2\pi J_0(w) \quad \text{and} \quad \int w J_0(w)\, dw = w J_1(w).$$

$$\int_{0+\gamma}^{2\pi+\gamma} e^{jw\cos\phi'} d\phi'$$

for any $\gamma \in R$

In this section we have considered the radiation properties of only relatively simple cases of rectangular and circular apertures in conducting planes. The analysis of other aperture-type antennas such as horns, reflectors, and lenses is more difficult and requires the use of more advanced concepts. Slots cut in the walls of a waveguide that interrupt current flow will radiate. Suitably arranged, they will form antenna arrays in a manner analogous to dipole arrays. These and other radiation problems are topics for more specialized books on antennas [9], [11] [13].

References

[1] H. Unz, "Linear arrays with arbitrarily distributed elements," *IRE Transactions on Antennas and Propagation*, vol. AP-8, pp. 222–223, March 1960.

[2] R. F. Harrington, "Sidelobe reduction by nonuniform element spacing," *IRE Transactions on Antennas and Propagation*, vol. AP-9, pp. 187–192, March 1961.

[3] A. Ishimaru and Y. S. Chen, "Thinning and broadbanding antenna arrays by unequal spacings," *IEEE Transactions on Antennas and Propagation*, vol. AP-13, pp. 34–42, January 1965.

[4] F. I. Tseng and D. K. Cheng, "Spacing perturbation techniques for array optimization," *Radio Science*, vol. 3 (New Series), pp. 451–457, May 1968.

[5] D. K. Cheng and P. D. Raymond, Jr., "Optimization of array directivity by phase adjustments," *Electronics Letters*, vol. 7, pp. 552–553, September 9, 1971.

[6] E. D. Sharp, "A triangular arrangement of planar array elements that reduces the number needed," *IRE Transactions on Antennas and Propagation*, vol. AP-9, pp. 126–129, March 1961.

[7] N. Goto, "Pattern synthesis of hexagonal planar array," *IEEE Transactions on Antennas and Propagation*, vol. AP-20, pp. 104–106, January 1972.

[8] D. K. Cheng, "Optimization techniques for antenna arrays," *Proceedings of the IEEE*, vol. 59, pp. 1664–1674, December 1971.

[9] E. C. Jordan and K. G. Balmain, *Electromagnetic Waves and Radiating Systems*, Prentice-Hall, Englewood Cliffs, N.J., 1968.

[10] M. T. Ma, *Theory and Application of Antenna Arrays*, Wiley, New York, 1974.

[11] R. S. Elliott, *Antenna Theory and Design*, Prentice-Hall, Englewood Cliffs, N.J., 1981.

[12] W. L. Stutzman and G. A. Thiele, *Antenna Theory and Design*, Wiley, New York, 1981.

[13] R. E. Collin, *Antennas and Radiowave Propagation*, McGraw-Hill, New York, 1985.

[14] K. F. Lee, *Principles of Antenna Theory*, Wiley, New York, 1984.

[15] H. Yagi, "Beam transmission of ultra short waves," *Proceedings of the IEEE*, vol. 16, pp. 715–741, June 1928.

[16] S. Uda and Y. Mushiaki, *Yagi-Uda Antenna*, Maruzan, Tokyo, 1954.

[17] D. K. Cheng and C. A. Chen, "Optimum element spacings for Yagi-Uda arrays," *IEEE Transactions on Antennas and Propagation*, vol. AP-21, pp. 615–623, September 1973.

[18] C. A. Chen and D. K. Cheng, "Optimum element lengths for Yagi-Uda arrays," *IEEE Transactions on Antennas and Propagation*, vol. AP-23, pp. 8–15, January 1975.

[19] V. H. Rumsey, *Frequency-Independent Antennas*, Academic Press, New York, 1966.

[20] J. D. Dyson, "The equiangular spiral," *IRE Transactions on Antennas and Propagation*, vol. AP-7, pp. 181–187, April 1959.

[21] R. H. DuHamel and D. E. Isbell, "Broadband logarithmically periodic antenna structures," *IRE National Convention Record*, Part I, pp. 119–128, 1957.
[22] R. H. DuHamel and F. R. Ore, "Logarithmically periodic antenna design," *IRE National Convention Record*, Part I, pp. 139–151, 1958.
[23] R. Carrel, "The design of log-periodic dipole antennas," *IRE International Convention Record*, Part I, pp. 61–75, 1961.
[24] E. C. Jordan et al., "Developments in broadband antennas," *IEEE Spectrum*, vol. 1, pp. 58–71, April 1964.
[25] S. Silver (ed.), *Microwave Antenna Theory and Design*, M.I.T. Radiation Laboratory Series, vol. 12, Chapters 5 and 6, McGraw-Hill, New York, 1949.

Review Questions

R.11–1 Give a general definition for *antenna*.

R.11–2 Why are antennas important for wireless communication over long distances?

R.11–3 State the procedure for finding the electromagnetic field due to an assumed time-harmonic current distribution on an antenna structure.

R.11–4 What is a *Hertzian dipole*?

R.11–5 What constitutes an elemental magnetic dipole?

R.11–6 Define the *near zone* and the *far zone* of an antenna.

R.11–7 Why are the near-zone fields called quasi-static fields?

R.11–8. Explain how the magnitude of far fields varies with distance.

R.11–9 In what ways does the electromagnetic field of a radiating magnetic dipole differ from that of a Hertzian dipole?

R.11–10 What are *radiation fields*?

R.11–11 Define *antenna pattern*.

R.11–12 Describe the E-plane and H-plane patterns of a Hertzian dipole.

R.11–13 Define *beamwidth* of an antenna pattern.

R.11–14 Define *sidelobe level* of an antenna pattern.

R.11–15 Define *radiation intensity*.

R.11–16 Define *directive gain* and *directivity* of an antenna.

R.11–17 Define *power gain* and *radiation efficiency* of an antenna.

R.11–18 Define *radiation resistance* of an antenna.

R.11–19 Discuss how the ratios (a/λ) and $(d\ell/\lambda)$ of a Hertzian dipole affect its radiation resistance and radiation efficiency.

R.11–20 Describe the radiation pattern of a half-wave dipole antenna.

R.11–21 What are the radiation resistance and directivity of a half-wave dipole antenna?

R.11–22 What is the image of a horizontal dipole over a conducting ground?

R.11–23 What are the radiation resistance and directivity of a vertical quarter-wave monopole over a conducting ground?

10

Waveguides and Cavity Resonators

10–1 Introduction

In the preceding chapter we studied the characteristic properties of transverse electromagnetic (TEM) waves guided by transmission lines. The TEM mode of guided waves is one in which the electric and magnetic fields are perpendicular to each other and both are transverse to the direction of propagation along the guiding line. One of the salient properties of TEM waves guided by conducting lines of negligible resistance is that the velocity of propagation of a wave of any frequency is the same as that in an unbounded dielectric medium. This was pointed out in connection with Eq. (9–21) and was reinforced by Eq. (9–72).

TEM waves, however, are not the only mode of guided waves that can propagate on transmission lines; nor are the three types of transmission lines (parallel-plate, two-wire, and coaxial) mentioned in Section 9–1 the only possible wave-guiding structures. As a matter of fact, we see from Eqs. (9–55) and (9–63) that the attenuation constant resulting from the finite conductivity of the lines increases with R, the resistance per unit line length, which, in turn, is proportional to $\sqrt{f}$ in accordance with Tables 9–1 and 9–2. Hence the attenuation of TEM waves tends to increase monotonically with frequency and would be prohibitively high in the microwave range.

In this chapter we first present a general analysis of the characteristics of the waves propagating along uniform guiding structures. Waveguiding structures are called ***waveguides***, of which the three types of transmission lines are special cases. The basic governing equations will be examined. We will see that, in addition to ***transverse electromagnetic (TEM) waves***, which have no field components in the direction of propagation, both ***transverse magnetic (TM) waves*** with a longitudinal electric-field component and ***transverse electric (TE) waves*** with a longitudinal magnetic-field component can also exist. Both TM and TE modes have characteristic ***cutoff frequencies***. Waves of frequencies below the cutoff frequency of a particular mode cannot propagate, and power and signal transmission at that mode is possible

only for frequencies higher than the cutoff frequency. Thus waveguides operating in TM and TE modes are like high-pass filters.

Also in this chapter we will reexamine the field and wave characteristics of parallel-plate waveguides with emphasis on TM and TE modes and show that all transverse field components can be expressed in terms of E_z (z being the direction of propagation) for TM waves and in terms of H_z for TE waves. The attenuation constants resulting from imperfectly conducting walls will be determined for TM and TE waves, and we will find that the attenuation constant depends, in a complicated way, on the mode of the propagating wave, as well as on frequency. For some modes the attenuation may decrease as the frequency increases; for other modes the attenuation may reach a minimum as the frequency exceeds the cutoff frequency by a certain amount.

Electromagnetic waves can propagate through hollow metal pipes of an arbitrary cross section. Without electromagnetic theory it would not be possible to explain the properties of hollow waveguides. We will see that single-conductor waveguides cannot support TEM waves. We will examine in detail the fields, the current and charge distributions, and the propagation and attenuation characteristics of rectangular and circular cylindrical waveguides. Both TM and TE modes will be discussed.

Electromagnetic waves can also be guided by an open dielectric-slab waveguide. The fields are essentially confined within the dielectric region and decay rapidly away from the slab surface in the transverse plane. For this reason the waves supported by a dielectric-slab waveguide are called ***surface waves***. Both TM and TE modes are possible. We will examine the field characteristics and cutoff frequencies of those surface waves. Cylindrical optical fibers will also be discussed.

At microwave frequencies, ordinary lumped-parameter elements (such as inductances and capacitances) connected by wires are no longer practical as circuit elements or as resonant circuits because the dimensions of the elements would have to be extremely small, because the resistance of the wire circuits becomes very high as a result of the skin effect, and because of radiation. We will briefly discuss irises and posts as waveguide reactive elements. A hollow conducting box with proper dimensions can be used as a resonant device. The box walls provide large areas for current flow, and losses are extremely small. Consequently, an enclosed conducting box can be a resonator of a very high Q. Such a box, which is essentially a segment of a waveguide with closed end faces, is called a ***cavity resonator***. We will discuss the different mode patterns of the fields inside rectangular as well as circular cylindrical cavity resonators.

10–2 General Wave Behaviors along Uniform Guiding Structures

In this section we examine some general characteristics for waves propagating along straight guiding structures with a uniform cross section. We will assume that the waves propagate in the $+z$-direction with a propagation constant $\gamma = \alpha + j\beta$ that is yet to be determined. For harmonic time dependence with an angular frequency ω, the dependence on z and t for all field components can be described by the exponential

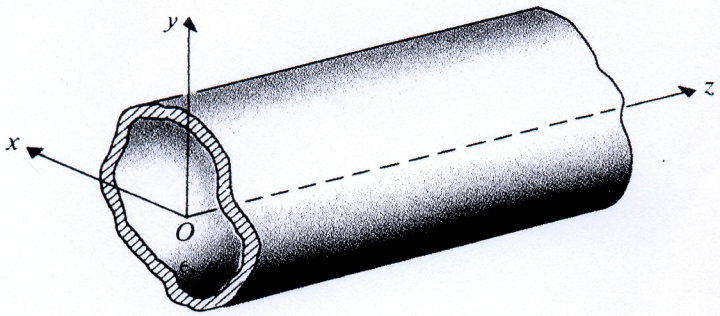

FIGURE 10–1
A uniform waveguide with an arbitrary cross section.

factor

$$e^{-\gamma z}e^{j\omega t} = e^{(j\omega t - \gamma z)} = e^{-\alpha z}e^{j(\omega t - \beta z)}. \tag{10–1}$$

As an example, for a cosine reference we may write the instantaneous expression for the **E** field in Cartesian coordinates as

$$\mathbf{E}(x, y, z; t) = \mathscr{R}e[\mathbf{E}^0(x, y)e^{(j\omega t - \gamma z)}], \tag{10–2}$$

where $\mathbf{E}^0(x, y)$ is a two-dimensional vector phasor that depends only on the cross-sectional coordinates. The instantaneous expression for the **H** field can be written in a similar way. Hence, in using a phasor representation in equations relating field quantities we may replace partial derivatives with respect to t and z simply by products with $(j\omega)$ and $(-\gamma)$, respectively; the common factor $e^{(j\omega t - \gamma z)}$ can be dropped.

We consider a straight waveguide in the form of a dielectric-filled metal tube having an arbitrary cross section and lying along the z-axis, as shown in Fig. 10–1. According to Eqs. (7–105) and (7–106), the electric and magnetic field intensities in the charge-free dielectric region inside satisfy the following homogeneous vector Helmholtz's equations:

$$\nabla^2\mathbf{E}^0 + k^2\mathbf{E}^0 = 0 \tag{10–3}$$

and

$$\nabla^2\mathbf{H}^0 + k^2\mathbf{H}^0 = 0, \tag{10–4}$$

where **E** and **H** are three-dimensional vector phasors, and k is the wavenumber:

$$k = \omega\sqrt{\mu\epsilon}. \tag{10–5}$$

The three-dimensional Laplacian operator ∇^2 may be broken into two parts: $\nabla^2_{u_1u_2}$ for the cross-sectional coordinates and ∇^2_z for the longitudinal coordinate. For waveguides with a rectangular cross section we use Cartesian coordinates:

$$\begin{aligned}\nabla^2\mathbf{E} &= (\nabla^2_{xy} + \nabla^2_z)\mathbf{E} = \left(\nabla^2_{xy} + \frac{\partial^2}{\partial z^2}\right)\mathbf{E} \\ &= \nabla^2_{xy}\mathbf{E} + \gamma^2\mathbf{E}.\end{aligned} \tag{10–6}$$

Combination of Eqs. (10–3) and (10–6) gives

$$\nabla^2_{xy}\mathbf{E}^0 + (\gamma^2 + k^2)\mathbf{E}^0 = 0. \tag{10–7}$$

Similarly, from Eq. (10–4) we have

$$\nabla_{xy}^2 \mathbf{H}^{\circ} + (\gamma^2 + k^2)\mathbf{H}^{\circ} = 0. \tag{10–8}$$

We note that each of Eqs. (10–7) and (10–8) is really three second-order partial differential equations, one for each component of **E** and **H**. The exact solution of these component equations depends on the cross-sectional geometry and the boundary conditions that a particular field component must satisfy at conductor-dielectric interfaces. We note further that by writing $\nabla_{r\phi}^2$ for the transversal operator ∇_{xy}^2, Eqs. (10–7) and (10–8) become the governing equations for waveguides with a circular cross section.

Of course, the various components of **E** and **H** are not all independent, and it is not necessary to solve all six second-order partial differential equations for the six components of **E** and **H**. Let us examine the interrelationships among the six components in Cartesian coordinates by expanding the two source-free curl equations, Eqs. (7–104a) and (7–104b):

From $\nabla \times \mathbf{E} = -j\omega\mu\mathbf{H}$:		From $\nabla \times \mathbf{H} = j\omega\epsilon\mathbf{E}$:	
$\dfrac{\partial E_z^0}{\partial y} + \gamma E_y^0 = -j\omega\mu H_x^0$	(10–9a)	$\dfrac{\partial H_z^0}{\partial y} + \gamma H_y^0 = j\omega\epsilon E_x^0$	(10–10a)
$-\gamma E_x^0 - \dfrac{\partial E_z^0}{\partial x} = -j\omega\mu H_y^0$	(10–9b)	$-\gamma H_x^0 - \dfrac{\partial H_z^0}{\partial x} = j\omega\epsilon E_y^0$	(10–10b)
$\dfrac{\partial E_y^0}{\partial x} - \dfrac{\partial E_x^0}{\partial y} = -j\omega\mu H_z^0$	(10–9c)	$\dfrac{\partial H_y^0}{\partial x} - \dfrac{\partial H_x^0}{\partial y} = j\omega\epsilon E_z^0$	(10–10c)

Note that partial derivatives with respect to z have been replaced by multiplications by $(-\gamma)$. All the component field quantities in the equations above are phasors that depend only on x and y, the common $e^{-\gamma z}$ factor for z-dependence having been omitted. By manipulating these equations we can express the transverse field components H_x^0, H_y^0, and E_x^0, and E_y^0 in terms of the two longitudinal components E_z^0 and H_z^0. For instance, Eqs. (10–9a) and (10–10b) can be combined to eliminate E_y^0 and obtain H_x^0 in terms of E_z^0 and H_z^0. We have

$$H_x^0 = -\frac{1}{h^2}\left(\gamma \frac{\partial H_z^0}{\partial x} - j\omega\epsilon \frac{\partial E_z^0}{\partial y}\right), \tag{10–11}$$

$$H_y^0 = -\frac{1}{h^2}\left(\gamma \frac{\partial H_z^0}{\partial y} + j\omega\epsilon \frac{\partial E_z^0}{\partial x}\right), \tag{10–12}$$

$$E_x^0 = -\frac{1}{h^2}\left(\gamma \frac{\partial E_z^0}{\partial x} + j\omega\mu \frac{\partial H_z^0}{\partial y}\right), \tag{10–13}$$

$$E_y^0 = -\frac{1}{h^2}\left(\gamma \frac{\partial E_z^0}{\partial y} - j\omega\mu \frac{\partial H_z^0}{\partial x}\right), \tag{10–14}$$

where

$$h^2 = \gamma^2 + k^2. \tag{10-15}$$

The wave behavior in a waveguide can be analyzed by solving Eqs. (10–7) and (10–8) for the longitudinal components, E_z^0 and H_z^0, respectively, subject to the required boundary conditions, and then by using Eqs. (10–11) through (10–14) to determine the other components.

It is convenient to classify the propagating waves in a uniform waveguide into three types according to whether E_z or H_z exists.

1. *Transverse electromagnetic (TEM) waves.* These are waves that contain neither E_z nor H_z. We encountered TEM waves in Chapter 8 when we discussed plane waves and in Chapter 9 on waves along transmission lines.
2. *Transverse magnetic (TM) waves.* These are waves that contain a nonzero E_z but $H_z = 0$.
3. *Transverse electric (TE) waves.* These are waves that contain a nonzero H_z but $E_z = 0$.

The propagation characteristics of the various types of waves are different; they will be discussed in subsequent subsections.

10–2.1 TRANSVERSE ELECTROMAGNETIC WAVES

Since $E_z = 0$ and $H_z = 0$ for TEM waves within a guide, we see that Eqs. (10–11) through (10–14) constitute a set of trivial solutions (all field components vanish) unless the denominator h^2 also equals zero. In other words, TEM waves exist only when

$$\gamma_{\text{TEM}}^2 + k^2 = 0 \tag{10-16}$$

or

$$\gamma_{\text{TEM}} = jk = j\omega\sqrt{\mu\epsilon}, \tag{10-17}$$

which is exactly the same expression for the propagation constant of a uniform plane wave in an unbounded medium characterized by constitutive parameters ϵ and μ. We recall that Eq. (10–17) also holds for a TEM wave on a lossless transmission line. It follows that the velocity of propagation (phase velocity) for TEM waves is

$$\boxed{u_{p(\text{TEM})} = \frac{\omega}{k} = \frac{1}{\sqrt{\mu\epsilon}} \quad \text{(m/s)}.} \tag{10-18}$$

We can obtain the ratio between E_x^0 and H_y^0 from Eqs. (10–9b) and (10–10a) by setting E_z and H_z to zero. This ratio is called the ***wave impedance***. We have

$$Z_{\text{TEM}} = \frac{E_x^0}{H_y^0} = \frac{j\omega\mu}{\gamma_{\text{TEM}}} = \frac{\gamma_{\text{TEM}}}{j\omega\epsilon}, \tag{10-19}$$

which becomes, in view of Eq. (10–17),

$$\boxed{Z_{\text{TEM}} = \sqrt{\frac{\mu}{\epsilon}} = \eta \qquad (\Omega).} \tag{10–20}$$

We note that Z_{TEM} is the same as the intrinsic impedance of the dielectric medium, as given in Eq. (8–30). Equations (10–18) and (10–20) assert that ***the phase velocity and the wave impedance for TEM waves are independent of the frequency of the waves.***

Letting $E_z^0 = 0$ in Eq. (10–9a) and $H_z^0 = 0$ in Eq. (10–10b), we obtain

$$\frac{E_y^0}{H_x^0} = -Z_{\text{TEM}} = -\sqrt{\frac{\mu}{\epsilon}}. \tag{10–21}$$

Equations (10–19) and (10–21) can be combined to obtain the following formula for a TEM wave propagating in the $+z$-direction:

$$\boxed{\mathbf{H} = \frac{1}{Z_{\text{TEM}}}\,\mathbf{a}_z \times \mathbf{E} \qquad (\text{A/m}),} \tag{10–22}$$

which again reminds us of a similar relation for a uniform plane wave in an unbounded medium—see Eq. (8–29).

Single-conductor waveguides cannot support TEM waves. In Section 6–2 we pointed out that magnetic flux lines always close upon themselves. Hence if a TEM wave were to exist in a waveguide, the field lines of **B** and **H** would form closed loops in a transverse plane. However, the generalized Ampère's circuital law, Eq. (7–54b), requires that the line integral of the magnetic field (the magnetomotive force) around any closed loop in a transverse plane must equal the sum of the longitudinal conduction and displacement currents through the loop. Without an inner conductor there is no longitudinal conduction current inside the waveguide. By definition, a TEM wave does not have an E_z-component; consequently, there is no longitudinal displacement current. The total absence of a longitudinal current inside a waveguide leads to the conclusion that there can be no closed loops of magnetic field lines in any transverse plane. Therefore, we conclude that ***TEM waves cannot exist in a single-conductor hollow (or dielectric-filled) waveguide of any shape.*** On the other hand, *assuming perfect conductors*, a coaxial transmission line having an inner conductor *can* support TEM waves; so can a two-conductor stripline and a two-wire transmission line. When the conductors have losses, waves along transmission lines are strictly no longer TEM, as noted in Section 9–2.

10–2.2 TRANSVERSE MAGNETIC WAVES

Transverse magnetic (TM) waves do not have a component of the magnetic field in the direction of propagation, $H_z = 0$. The behavior of TM waves can be analyzed

by solving Eq. (10–7) for E_z subject to the boundary conditions of the guide and using Eqs. (10–11) through (10–14) to determine the other components. Writing Eq. (10–7) for E_z, we have

$$\nabla_{xy}^2 E_z^0 + (\gamma^2 + k^2)E_z^0 = 0 \tag{10–23}$$

or

$$\boxed{\nabla_{xy}^2 E_z^0 + h^2 E_z^0 = 0.} \tag{10–24}$$

Equation (10–24) is a second-order partial differential equation, which can be solved for E_z^0. In this section we wish to discuss only the general properties of the various wave types. The actual solution of Eq. (10–24) will wait until subsequent sections when we examine particular waveguides.

For TM waves we set $H_z = 0$ in Eqs. (10–11) through (10–14) to obtain

$$H_x^0 = \frac{j\omega\epsilon}{h^2}\frac{\partial E_z^0}{\partial y}, \tag{10–25}$$

$$H_y^0 = -\frac{j\omega\epsilon}{h^2}\frac{\partial E_z^0}{\partial x}, \tag{10–26}$$

$$E_x^0 = -\frac{\gamma}{h^2}\frac{\partial E_z^0}{\partial x}, \tag{10–27}$$

$$E_y^0 = -\frac{\gamma}{h^2}\frac{\partial E_z^0}{\partial y}. \tag{10–28}$$

It is convenient to combine Eqs. (10–27) and (10–28) and write

$$\boxed{(\mathbf{E}_T^0)_{\text{TM}} = \mathbf{a}_x E_x^0 + \mathbf{a}_y E_y^0 = -\frac{\gamma}{h^2}\nabla_T E_z^0 \qquad \text{(V/m)},} \tag{10–29}$$

where

$$\nabla_T E_z^0 = \left(\mathbf{a}_x \frac{\partial}{\partial x} + \mathbf{a}_y \frac{\partial}{\partial y}\right) E_z^0 \tag{10–30}$$

denotes the gradient of E_z^0 in the transverse plane. Equation (10–29) is a concise formula for finding E_x^0 and E_y^0 from E_z^0.

The transverse components of magnetic field intensity, H_x^0 and H_y^0, can be determined simply from E_x^0 and E_y^0 on the introduction of the wave impedance for the TM mode. We have, from Eqs. (10–25) through (10–28),

$$\boxed{Z_{\text{TM}} = \frac{E_x^0}{H_y^0} = -\frac{E_y^0}{H_x^0} = \frac{\gamma}{j\omega\epsilon} \qquad (\Omega).} \tag{10–31}$$

It is important to note that Z_{TM} is *not* equal to $j\omega\mu/\gamma$, because γ for TM waves, unlike γ_{TEM}, is *not* equal to $j\omega\sqrt{\mu\epsilon}$. The following relation between the electric and magnetic

field intensities holds for TM waves:

$H_z = 0 \Rightarrow$

$$\mathbf{H} = \frac{1}{Z_{TM}}(\mathbf{a}_z \times \mathbf{E}) \quad \text{(A/m)}. \tag{10–32}$$

Equation (10–32) is seen to be of the same form as Eq. (10–22) for TEM waves.

When we undertake to solve the two-dimensional homogeneous Helmholtz equation, Eq. (10–24), subject to the boundary conditions of a given waveguide, we will discover that solutions are possible only for *discrete values of h*. There may be an infinity of these discrete values, but solutions are not possible for all values of h. The values of h for which a solution of Eq. (10–24) exists are called the ***characteristic values*** or ***eigenvalues*** of the boundary-value problem. Each of the eigenvalues determines the characteristic properties of a particular TM mode of the given waveguide.

In the following sections we will also discover that the eigenvalues of the various waveguide problems are real numbers. From Eq. (10–15) we have

$$\begin{aligned}\gamma &= \sqrt{h^2 - k^2} \\ &= \sqrt{h^2 - \omega^2\mu\epsilon}.\end{aligned} \tag{10–33}$$

Two distinct ranges of the values for the propagation constant are noted, the dividing point being $\gamma = 0$, where

$$\omega_c^2\mu\epsilon = h^2 \tag{10–34}$$

or

$$f_c = \frac{h}{2\pi\sqrt{\mu\epsilon}} \quad \text{(Hz)}. \tag{10–35}$$

The frequency, f_c, at which $\gamma = 0$ is called a ***cutoff frequency***. *The value of f_c for a particular mode in a waveguide depends on the eigenvalue of this mode.* Using Eq. (10–35), we can write Eq. (10–33) as

$$\gamma = h\sqrt{1 - \left(\frac{f}{f_c}\right)^2}. \tag{10–36}$$

The two distinct ranges of γ can be defined in terms of the ratio $(f/f_c)^2$ as compared to unity.

a) $\left(\dfrac{f}{f_c}\right)^2 > 1$, or $f > f_c$. In this range, $\omega^2\mu\epsilon > h^2$ and γ is imaginary. We have, from Eq. (10–33),

$$\gamma = j\beta = jk\sqrt{1 - \left(\frac{h}{k}\right)^2} = jk\sqrt{1 - \left(\frac{f_c}{f}\right)^2}. \tag{10–37}$$

It is a propagating mode with a phase constant β:

$$\boxed{\beta = k\sqrt{1-\left(\frac{f_c}{f}\right)^2} \quad \text{(rad/m)}.} \tag{10-38}$$

The corresponding wavelength in the guide is

$$\lambda_g = \frac{2\pi}{\beta} = \frac{\lambda}{\sqrt{1-(f_c/f)^2}} > \lambda, \tag{10-39}$$

where

$$\lambda = \frac{2\pi}{k} = \frac{1}{f\sqrt{\mu\epsilon}} = \frac{u}{f} \tag{10-40}$$

is the wavelength of a plane wave with a frequency f in an unbounded dielectric medium characterized by μ and ϵ, and $u = 1/\sqrt{\mu\epsilon}$ is the velocity of light in the medium. Equation (10–39) can be rearranged to give a simple relation connecting λ, the guide wavelength λ_g, and the cutoff wavelength $\lambda_c = u/f_c$:

$$\frac{1}{\lambda^2} = \frac{1}{\lambda_g^2} + \frac{1}{\lambda_c^2}. \tag{10-41}$$

The phase velocity of the propagating wave in the guide is

$$u_p = \frac{\omega}{\beta} = \frac{u}{\sqrt{1-(f_c/f)^2}} = \frac{\lambda_g}{\lambda}u > u. \tag{10-42}$$

We see from Eq. (10–42) that the phase velocity within a waveguide is always higher than that in an unbounded medium and is frequency-dependent. Hence ***single-conductor waveguides are dispersive transmission systems***, although an unbounded lossless dielectric medium is nondispersive. The group velocity for a propagating wave in a waveguide can be determined by using Eq. (8–72):

$$u_g = \frac{1}{d\beta/d\omega} = u\sqrt{1-\left(\frac{f_c}{f}\right)^2} = \frac{\lambda}{\lambda_g}u < u. \tag{10-43}$$

Thus,

$$u_g u_p = u^2. \tag{10-44}$$

For air dielectric, $u = c$, Eq. (10–44) becomes $u_g u_p = c^2$. In a lossless waveguide the velocity of signal propagation (the *velocity of energy transport*) is equal to the group velocity. An illustration of this statement can be found later, in Subsection 10–3.3.

Substitution of Eq. (10–37) in Eq. (10–31) yields

$$\boxed{Z_{\text{TM}} = \eta\sqrt{1-\left(\frac{f_c}{f}\right)^2} \quad (\Omega).} \tag{10-45}$$

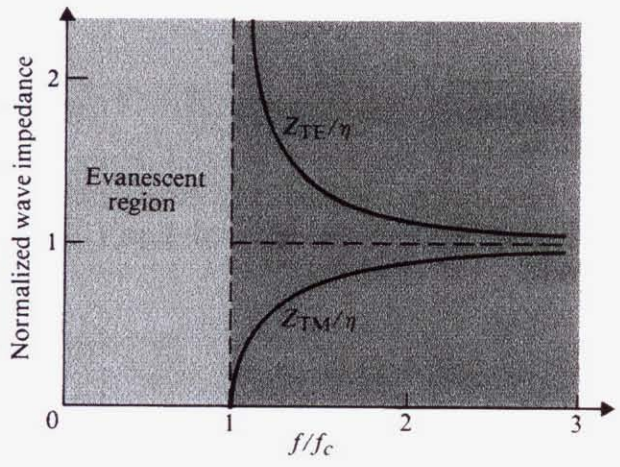

FIGURE 10–2
Normalized wave impedances for propagating TM and TE waves.

The wave impedance of propagating TM modes in a waveguide with a lossless dielectric is purely resistive and is always less than the intrinsic impedance of the dielectric medium. The variation of Z_{TM} versus f/f_c for $f > f_c$ is sketched in Fig. 10–2.

b) $\left(\frac{f}{f_c}\right)^2 < 1$, or $f < f_c$. When the operating frequency is lower than the cutoff frequency, γ is real and Eq. (10–36) can be written as

$$\gamma = \alpha = h\sqrt{1 - \left(\frac{f}{f_c}\right)^2}, \qquad f < f_c, \tag{10–46}$$

which is, in fact, an attenuation constant. Since all field components contain the propagation factor $e^{-\gamma z} = e^{-\alpha z}$, the wave diminishes rapidly with z and is said to be ***evanescent***. Therefore, ***a waveguide exhibits the property of a high-pass filter***. *For a given mode, only waves with a frequency higher than the cutoff frequency of the mode can propagate in the guide.*

Substitution of Eq. (10–46) in Eq. (10–31) gives the wave impedance of TM modes for $f < f_c$:

$$Z_{TM} = -j\frac{h}{\omega\epsilon}\sqrt{1 - \left(\frac{f}{f_c}\right)^2}, \qquad f < f_c. \tag{10–47}$$

Thus, the wave impedance of evanescent TM modes at frequencies below cutoff is purely reactive, indicating that there is no power flow associated with evanescent waves.

10–2.3 TRANSVERSE ELECTRIC WAVES

Transverse electric (TE) waves do not have a component of the electric field in the direction of propagation, $E_z = 0$. The behavior of TE waves can be analyzed by first

solving Eq. (10–8) for H_z:

$$\boxed{\nabla_{xy}^2 H_z + h^2 H_z = 0.} \tag{10–48}$$

Proper boundary conditions at the guide walls must be satisfied. The transverse field components can then be found by substituting H_z into the reduced Eqs. (10–11) through (10–14) with E_z set to zero. We have

$$H_x^0 = -\frac{\gamma}{h^2}\frac{\partial H_z^0}{\partial x}, \tag{10–49}$$

$$H_y^0 = -\frac{\gamma}{h^2}\frac{\partial H_z^0}{\partial y}, \tag{10–50}$$

$$E_x^0 = -\frac{j\omega\mu}{h^2}\frac{\partial H_z^0}{\partial y}, \tag{10–51}$$

$$E_y^0 = \frac{j\omega\mu}{h^2}\frac{\partial H_z^0}{\partial x}. \tag{10–52}$$

Combining Eqs. (10–49) and (10–50), we obtain

$$\boxed{(\mathbf{H}_T^0)_{TE} = \mathbf{a}_x H_x^0 + \mathbf{a}_y H_y^0 = -\frac{\gamma}{h^2}\nabla_T H_z^0 \qquad \text{(A/m)}.} \tag{10–53}$$

We note that Eq. (10–53) is entirely similar to Eq. (10–29) for TM modes.

The transverse components of electric field intensity, E_x^0 and E_y^0, are related to those of magnetic field intensity through the wave impedance. We have, from Eqs. (10–49) through (10–52),

$$\boxed{Z_{\text{TE}} = \frac{E_x^0}{H_y^0} = -\frac{E_y^0}{H_x^0} = \frac{j\omega\mu}{\gamma} \qquad (\Omega).} \tag{10–54}$$

Note that Z_{TE} in Eq. (10–54) is quite different from Z_{TM} in Eq. (10–31) because γ for TE waves, unlike γ_{TEM}, is *not* equal to $j\omega\sqrt{\mu\epsilon}$. Equations (10–51), (10–52), and (10–54) can now be combined to give the following vector formula:

$E_z = 0 \Longrightarrow$

$$\boxed{\mathbf{E} = -Z_{\text{TE}}(\mathbf{a}_z \times \mathbf{H}) \qquad \text{(V/m)}.} \tag{10–55}$$

Inasmuch as we have not changed the relation between γ and h, Eqs. (10–33) through (10–44) pertaining to TM waves also apply to TE waves. There are also two distinct ranges of γ, depending on whether the operating frequency is higher or lower than the cutoff frequency, f_c, given in Eq. (10–35).

a) $\left(\frac{f}{f_c}\right)^2 > 1$, or $f > f_c$. In this range, γ is imaginary, and we have a propagating mode. The expression for γ is the same as that given in Eq. (10–37):

$$\gamma = j\beta = jk\sqrt{1 - \left(\frac{f_c}{f}\right)^2}. \tag{10–56}$$

Consequently, the formulas for β, λ_g, u_p, and u_g in Eqs. (10–38), (10–39), (10–42), and (10–43), respectively, also hold for TE waves. Using Eq. (10–56) in Eq. (10–54), we obtain

$$\boxed{Z_{TE} = \frac{\eta}{\sqrt{1 - (f_c/f)^2}} \quad (\Omega),} \tag{10–57}$$

which is obviously different from the expression for Z_{TM} in Eq. (10–45). Equation (10–57) indicates that ***the wave impedance of propagating TE modes in a waveguide with a lossless dielectric is purely resistive and is always larger than the intrinsic impedance of the dielectric medium***. The variation of Z_{TE} versus f/f_c for $f > f_c$ is also sketched in Fig. 10–2.

b) $\left(\frac{f}{f_c}\right)^2 < 1$, or $f < f_c$. In this case, γ is real and we have an evanescent or non-propagating mode:

$$\gamma = \alpha = h\sqrt{1 - \left(\frac{f}{f_c}\right)^2}, \qquad f < f_c. \tag{10–58}$$

Substitution of Eq. (10–58) in Eq. (10–54) gives the wave impedance of TE modes for $f < f_c$:

$$Z_{TE} = j\frac{\omega\mu}{h\sqrt{1 - (f/f_c)^2}}, \qquad f < f_c, \tag{10–59}$$

which is purely reactive, indicating again that there is no power flow for evanescent waves at $f < f_c$.

EXAMPLE 10–1 (a) Determine the wave impedance and guide wavelength at a frequency equal to twice the cutoff frequency in a waveguide for TM and TE modes. (b) Repeat part (a) for a frequency equal to one-half of the cutoff frequency. (c) What are the wave impedance and guide wavelength for the TEM mode?

Solution

a) At $f = 2f_c$, which is above the cutoff frequency, we have propagating modes. The appropriate formulas are Eqs. (10–45), (10–57), and (10–39).

For $f = 2f_c$, $(f_c/f)^2 = \frac{1}{4}$, $\sqrt{1 - (f_c/f)^2} = \sqrt{3}/2 = 0.866$. Thus,

$$Z_{TM} = 0.866\eta < \eta, \qquad \lambda_{TM} = 1.155\lambda > \lambda,$$
$$Z_{TE} = 1.155\eta > \eta, \qquad \lambda_{TE} = 1.155\lambda > \lambda,$$

TABLE 10–1
Wave Impedances and Guide Wavelengths for $f > f_c$

Mode	Wave Impedance, Z	Guide Wavelength, λ_g
TEM	$\eta = \sqrt{\dfrac{\mu}{\epsilon}}$	$\lambda = \dfrac{1}{f\sqrt{\mu\epsilon}}$
TM	$\eta\sqrt{1 - \left(\dfrac{f_c}{f}\right)^2}$	$\dfrac{\lambda}{\sqrt{1 - (f_c/f)^2}}$
TE	$\dfrac{\eta}{\sqrt{1 - (f_c/f)^2}}$	$\dfrac{\lambda}{\sqrt{1 - (f_c/f)^2}}$

where η is the intrinsic impedance of the guide medium. These results are summarized in Table 10–1.

b) At $f = f_c/2 < f_c$, the waveguide modes are evanescent, and guide wavelength has no significance. We now have

$$Z_{\text{TM}} = -j\frac{h}{\omega\epsilon}\sqrt{1 - \left(\frac{f}{f_c}\right)^2} = -j0.276h/f_c\epsilon,$$

$$Z_{\text{TE}} = j\frac{\omega\mu}{h\sqrt{1 - (f/f_c)^2}} = j3.63f_c\mu/h.$$

We note that both Z_{TM} and Z_{TE} become imaginary (reactive) for evanescent modes at $f < f_c$; their values depend on the eigenvalue h, which is a characteristic of the particular TM or TE mode.

c) The TEM mode does not exhibit a cutoff property and $h = 0$. The wave impedance and guide wavelength are independent of frequency. From Eqs. (10–20) and (10–18) we have

$$Z_{\text{TEM}} = \eta$$

and

$$\lambda_{\text{TEM}} = \lambda.$$

For propagating modes, $\gamma = j\beta$ and the variation of β versus frequency determines the characteristics of a wave along a guide. It is therefore useful to plot and examine an ω–β diagram.† Figure 10–3 is such a diagram in which the dashed line through the origin represents the ω–β relationship for TEM mode. The constant slope of this straight line is $\omega/\beta = u = 1/\sqrt{\mu\epsilon}$, which is the same as the velocity of light in an unbounded dielectric medium with constitutive parameters μ and ϵ.

† Also referred to as a ***Brillouin diagram***.

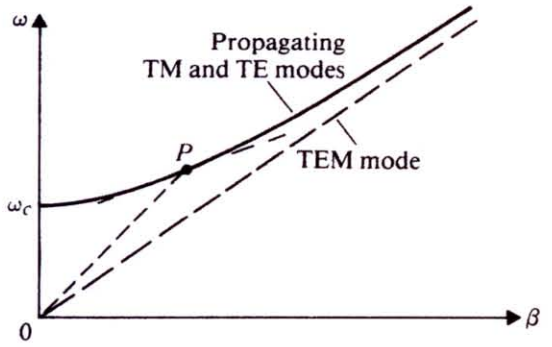

FIGURE 10–3
ω–β diagram for waveguide.

The solid curve above the dashed line depicts a typical ω–β relation for either a TM or a TE propagating mode, given by Eq. (10–38). We can write

$$\omega = \frac{\beta u}{\sqrt{1 - (\omega_c/\omega)^2}}. \tag{10–60}$$

The ω–β curve intersects the ω-axis ($\beta = 0$) at $\omega = \omega_c$. The slope of the line joining the origin and any point, such as P, on the curve is equal to the phase velocity, u_p, for a particular mode having a cutoff frequency f_c and operating at a particular frequency. The local slope of the ω–β curve at P is the group velocity, u_g. We note that, for propagating TM and TE waves in a waveguide, $u_p > u$, $u_g < u$, and Eq. (10–44) holds. As the operating frequency increases much above the cutoff frequency, both u_p and u_g approach u asymptotically. The exact value of ω_c depends on the eigenvalue h in Eq. (10–35)—that is, on the particular TM or TE mode in a waveguide of a given cross section. Methods for determining h will be discussed when we examine different types of waveguides. We recall that the ω–β graph for wave propagation in an ionized medium (Fig. 8–7) was quite similar to the ω–β diagram for a waveguide shown in Fig. 10–3.

EXAMPLE 10–2 Obtain a graph showing the relation between the attenuation constant α and the operating frequency f for evanescent modes in a waveguide.

Solution For evanescent TM or TE modes, $f < f_c$ and Eq. (10–46) or (10–58) applies. We have

$$\left(\frac{f_c}{h}\alpha\right)^2 + f^2 = f_c^2. \tag{10–61}$$

Hence the graph of $(f_c\alpha/h)$ plotted versus f is a circle centered at the origin and having a radius f_c. This is shown in Fig. 10–4. The value of α for any $f < f_c$ can be found from this quarter of a circle.

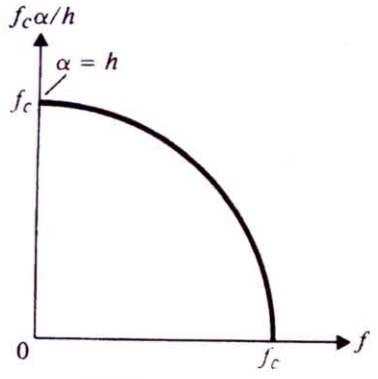

FIGURE 10–4
Relation between attenuation constant and operating frequency for evanescent modes (Example 10–2).

10–3 Parallel-Plate Waveguide

In Section 9–2 we discussed the characteristics of TEM waves propagating along a parallel-plate transmission line. It was then pointed out, and again emphasized in Subsection 10–2.1, that the field behavior for TEM modes bears a very close resemblance to that for uniform plane waves in an unbounded dielectric medium. However, TEM modes are not the only type of waves that can propagate along perfectly conducting parallel-plates separated by a dielectric. A parallel-plate waveguide can also support TM and TE waves. The characteristics of these waves are examined separately in following subsections.

10–3.1 TM WAVES BETWEEN PARALLEL PLATES

Consider the parallel-plate waveguide of two perfectly conducting plates separated by a dielectric medium with constitutive parameters ϵ and μ, as shown in Fig. 10–5. The plates are assumed to be infinite in extent in the x-direction. This is tantamount to assuming that the fields do not vary in the x-direction and that edge effects are negligible. Let us suppose that TM waves ($H_z = 0$) propagate in the $+z$-direction. For harmonic time dependence it is expedient to work with equations relating field

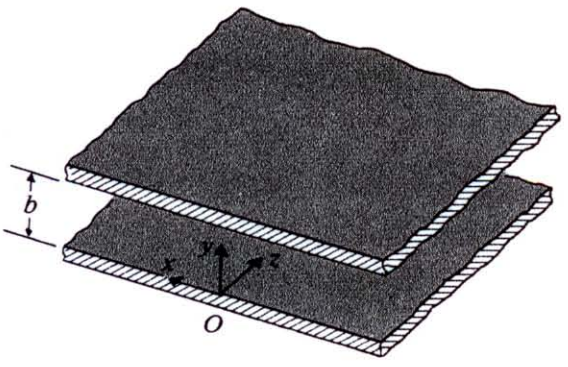

FIGURE 10–5
An infinite parallel-plate waveguide.